https://doi.org/10.5194/egusphere-2024-3375
Preprint. Discussion started: 6 November 2024
© Author(s) 2024. CC BY 4.0 License.

Developing a low-cost device for estimating air–water ΔpCO_2 in coastal environments

Elizabeth B. Farquhar[1,2], Philip J. Bresnahan[1,2], Michael Tydings[1,2], Jessie C. Jarvis[2,3], Robert F. Whitehead[2], Dan Portelli[1,2]

[1]Department of Earth and Ocean Sciences, University of North Carolina Wilmington, Wilmington, 28403, USA
[2]Center for Marine Science, University of North Carolina Wilmington, Wilmington, 28409, USA
[3]Department of Biology and Marine Biology, University of North Carolina Wilmington, Wilmington, 28403, USA

Correspondence to: Philip Bresnahan (bresnahanp@uncw.edu)

Abstract. The ocean is one of the world's largest anthropogenic carbon dioxide (CO_2) sinks, but closing the carbon budget is logistically difficult and expensive, and uncertainties in carbon fluxes and reservoirs remain. Specifically, measuring the CO_2 flux at the air–sea interface usually requires costly sensors or analyzers (>30,000 USD), which can limit what a group is able to monitor. Our group has developed and validated a low-cost ΔpCO_2 system for ~1,400 USD with Internet of Things (IoT) capabilities to combat this limitation using a ~100 USD pCO_2 K30 sensor at its core. Our Sensor for the Exchange of Atmospheric CO_2 with Water (SEACOW) may be placed in an observational network with traditional pCO_2 sensors to extend the spatial coverage and resolution of monitoring systems. After calibration, the SEACOW reports atmospheric pCO_2 measurements within 2–3% of measurements made by a calibrated LI-COR LI-850. We also demonstrate the SEACOW's ability to capture diel pCO_2 cycling in seagrass, provide recommendations for SEACOW field deployments, and provide additional technical specifications for the SEACOW and for the K30 itself (e.g., air and water-side 99.3% response time; 5.7 and 29.6 minutes, respectively).

1 Introduction

The ocean absorbs approximately 26% of the CO_2 emitted from human activities every year (Friedlingstein et al., 2022), demonstrating its critical role in buffering climate change. However, the ocean's ability to store carbon varies significantly based on temperature, habitat type, circulation patterns, organic carbon concentration, alkalinity, and more, exemplifying the complex nature of the carbon cycle. For instance, coastal environments with upwelling may be net sources and outgas CO_2 (Dai et al., 2022), while some habitats are net sinks, sequestering CO_2 (Bauer et al., 2013). Moreover, there is a large degree of temporal variability in carbon cycling in aquatic ecosystems, with some switching from a net sink to a net source or vice versa throughout the year (Takahashi et al., 1993; Lefèvre et al., 1999). Therefore, monitoring these habitats at a high spatial and temporal resolution is crucial to understanding their variable carbon budgets. Air–water CO_2 fluxes are one piece of the carbon budget that may offer insight into a given habitat's role in the ocean carbon cycle.

https://doi.org/10.5194/egusphere-2024-3375
Preprint. Discussion started: 6 November 2024
© Author(s) 2024. CC BY 4.0 License.

Seagrass meadows are one type of "blue carbon" ecosystem especially well studied for their role in carbon cycling. Despite only covering 0.2% of the ocean's surface, seagrass may be responsible for 10% of the organic carbon stored in the ocean (Herr and Landis, 2016; Fourqurean et al., 2012). However, these estimates were made using data compiled from around the globe, which can lack the spatial resolution needed to advise local management decisions (Fourqurean et al., 2012; Macreadie et al., 2014). Furthermore, modeling general coastal CO_2 uptakes rates can be difficult, with some models overestimating or underestimating rates (Resplandy et al., 2024; Watson et al., 2020), demonstrating the need for more direct measurements of the environments to inform such models.

Currently, air–water CO_2 fluxes are primarily measured by floating chambers, ΔpCO_2 devices (CO2-Pro Pro-Oceanus, Canada; 32,000 USD), aquatic pCO_2 devices that assume a spatially uniform atmospheric CO_2 (Takahashi et al., 2009), or eddy covariance instrumentation (LI-COR, Nebraska, USA; 26,500 USD) (Rosentreter, 2022). With high quality (and typically higher cost) devices or discrete sampling methodologies, it can be difficult to collect enough data to thoroughly resolve spatial variability. As a result, several groups have developed low-cost aquatic pCO_2 sensors, whose values can contribute to the estimation of CO_2 fluxes according to the following Eq. (1):

$$F = [k_w * K_H * \Delta pCO_2], \quad (1)$$

where k_w is the gas transfer velocity (m hr^{-1}), K_H is the solubility of CO_2 (mol m^{-3} atm^{-1}) which depends on pressure, temperature, and salinity, and ΔpCO_2 is (pCO_2^{water} – pCO_2^{air}) in atm (Wanninkhof, 1992; Wanninkhof et al., 2009). Several low-cost aquatic pCO_2 examples include the SIP-CO2 (Hunt et al., 2017) , the ACDC (Wall, 2014), the Gas-Pro (Graziani et al., 2014), and a fluorescent pCO_2 sensor (Ge et al., 2014). Additionally, the Fluxbot was developed as a low-cost CO_2 flux chamber, and although it is intended for terrestrial use, it is a notable example of low-cost CO_2 flux technology (Pan et al., 2024). Here we use 5,000 USD in 2024 dollars as a loose threshold for low cost. There are also several mid to high-range commercial pCO_2 sensors, including the Turner Designs C-Sense, the Pro-Oceanus CO2-Pro CV, the Pro-Oceanus Mini CO2, and the CONTROS HydroCR CO2 (7,000 – 20,000 USD at time of writing). Despite many pCO_2 options existing, we are not aware of other low-cost ΔpCO_2 devices, meaning able to measure both pCO_2^{water} and pCO_2^{air}. Several studies have built ΔpCO_2 systems using more expensive sensors and, frequently, onboard standards for autonomous calibration (Sabine et al., 2020; Nicholson et al., 2018; Sutton et al., 2014). A ΔpCO_2 device is especially advantageous because drift, or the gradual decrease in sensor accuracy, can theoretically be minimized, which is one of the greatest challenges with low-cost instrumentation. When taking the difference between pCO_2^{water} and pCO_2^{air}, the drift that has occurred on the sensor is subtracted out of the final ΔpCO_2, providing a more robust value (assuming that drift occurs as in the form of an offset that affects both water and air-side measurements equally) (Bresnahan Jr et al., 2014).

In this paper, we detail the creation of a low-cost internet of things (IoT) ΔpCO_2 device, termed the SEACOW, or System for the Exchange of Atmospheric CO_2 with Water, built for ~1,400 USD. We conducted laboratory and field investigations to rigorously characterize the SEACOW and its K30 CO_2 sensor (e.g., response time, accuracy, power budget, deployment length), as well as examined its ability to capture the diel cycling of pCO_2 due to seagrass productivity.

https://doi.org/10.5194/egusphere-2024-3375
Preprint. Discussion started: 6 November 2024
© Author(s) 2024. CC BY 4.0 License.

2 Methods and materials

2.1 Developing the SEACOW

2.1.1 Internal components

The SEACOW is designed to sit at the surface of the water, half submerged and with one CO_2 exchanger in the air and one in water. CO_2 permeates through expanded PTFE (ePTFE) membranes, enters an internal, sealed air stream, and flows through a solenoid valve, 24 in of nafion tubing placed inside ~160 g of Drierite desiccant, a gas pump, a 35 µm filter, and into a custom K30 housing, and finally to a second 3-way solenoid valve (Figure 1). Tubing was used for the water side of the SEACOW to decrease bubbles that could get trapped on the surface of the planar ePTFE when deployed.

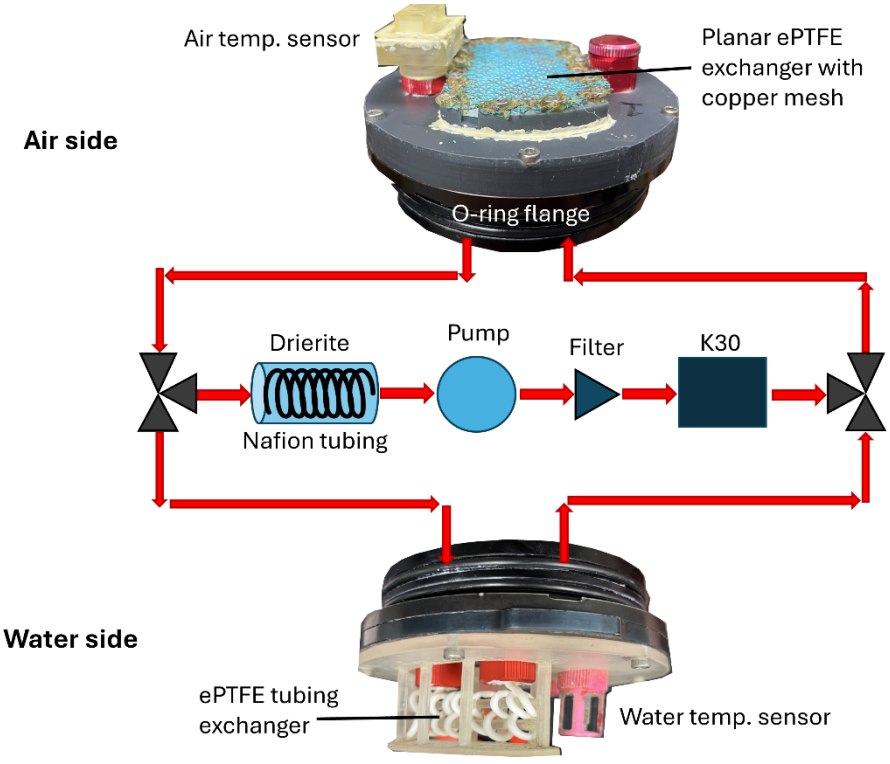

Figure 1. The plumbing diagram using ePTFE as a planar exchanger for the air-side and ePTFE tubing for the water-side. The use of ePTFE as the exchanger was inspired by methods used in previous studies (Johnson et al., 2009).

The K30 is a non-dispersive infrared (NDIR) CO_2 sensor (99 USD, Senseair, Sweden) with an accuracy of ±30 µatm ±3% of the reading, which can be improved significantly with calibration (Yasuda et al., 2012; Wall, 2014; Martin et al., 2017; Hunt et al., 2017). While the K30 manual states it measures XCO_2, it was empirically determined by Wall (2014) that the K30 measures pCO_2, with which our group concurred after preliminary testing (in other words, the readings are proportional to pressure). Additionally, the K30 has an automatic baseline correction (ABC) algorithm that helps to deter long term drift, which was turned off prior to deployments using methods described in the K30 Modbus manual (Senseair of Delsbo, 2023).

https://doi.org/10.5194/egusphere-2024-3375
Preprint. Discussion started: 6 November 2024
© Author(s) 2024. CC BY 4.0 License.

We incorporated the K30 into our system through its universal asynchronous receiver transmitter (UART) capabilities for serial communication. The K30 was encased in a custom 3D-printed housing and sealed with marine epoxy to ensure it was airtight (Figure 2). Additionally, we placed BME280 Sensor (Adafruit, NYC USA) inside the K30 housing to measure temperature, pressure, and humidity. The BME280 reads humidity with ±3% accuracy, barometric pressure with ±1 hPa absolute accuracy, and temperature with ±1.0 °C accuracy. All materials used to build the SEACOW are listed on our Github repository (https://zenodo.org/doi/10.5281/zenodo.13751037). Additionally, a circuit diagram of electrical components with part numbers is available in Appendix A.

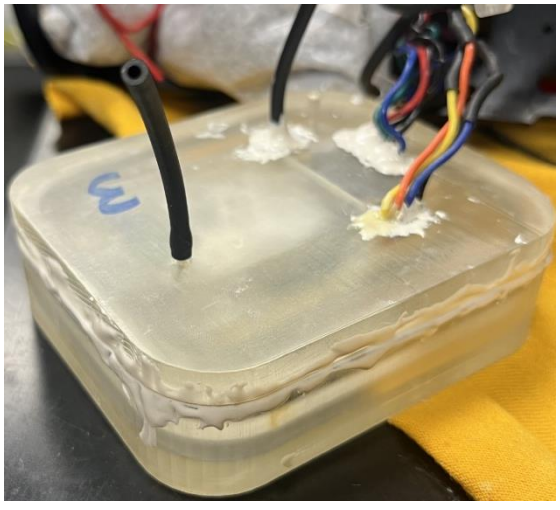

Figure 2. The 3D-printed K30 housing. The wire holes and top are sealed with marine epoxy. The BME 280 and K30 sensors are housed inside. It is 8.7 cm x 7.5 cm x 2.7 cm.

2.1.2 Outer housing

The entire interior system, including all its electrical components, was secured onto an electronics tray with zip ties that slides into a 4 in diameter schedule 80 PVC tube, which was polished to be o-ring smooth (600 grit emery cloth). On both ends of the PVC tube, there is a watertight end cap secured into place by an o-ring flange (Blue Robotics, CA, USA). For the 3D printed end cap on the air-side, we included a serpentine channel on it to increase the surface area of the exchanger's surface. The end cap is compatible with the existing o-ring flange from Blue Robotics after being polished. The ePTFE membrane (IPE, Arizona USA) is placed on top of the serpentine channel and secured in place using a 3D printed retainer and 4-40 machine screws (Figure 1). To measure air temperature, a TMP117 sensor (Adafruit, NYC USA) was placed inside a custom 3D printed housing that fits onto a Blue Robotics cable penetrator. The TMP117 is sealed into its housing using marine epoxy except for a small portion where the actual sensing component of the TMP117 is exposed, which was covered in thermally conductive epoxy in order to improve thermal response time.

https://doi.org/10.5194/egusphere-2024-3375
Preprint. Discussion started: 6 November 2024
© Author(s) 2024. CC BY 4.0 License.

For the water-side cap, we 3D printed a tubing holder that fits on top of the aluminum end cap from Blue Robotics. The 1.85 mm inner diameter ePTFE tubing (IPE, Arizona USA) was coiled around the 3D printed tubing holder and connected to two cable penetrators potted with barbed tubing and sealed with marine epoxy, which connects to the rest of the airstream (Figure 1). We placed a temperature sensor (I2C Fast Response, Blue Robotics) on this side to measure water temperature. All 3D designs, including the K30 housing, were printed in Formlabs clear resin on a Formlabs Form 3 printer, and are available on the SEACOW Github repository.

2.2 Characterizing the SEACOW

2.2.1 Air-side accuracy

Three additional SEACOWs were fabricated, and air-side measurements were compared between all four SEACOWs and those of a LI-850 (LI-COR Environmental, NE USA). To assess their readings at a range of CO_2 concentrations (0–1500 ppm), the rates of N_2 and CO_2 gas flowing into a sealed mixing chamber (~12 L) were varied, using calculations detailed in Appendix B and mass flow controllers. We increased the CO_2 concentration by increments of ~250 ppm every 25 minutes. The mixing chamber was connected to the inputs and outputs of the LI-850 and the SEACOWs. Using the equilibrated readings from each SEACOW and the LI-850 at each step of the experiment, we produced dry calibrations (slope and intercept from a linear regression) for each SEACOW after applying Eqs. (2-4), which are described below. The last 5 minutes of each step were considered the equilibrated values.

2.2.2 Response time

The LI-850 has a 90% response time of < 3.5 seconds which, for our purposes and relative to the slower K30 and SEACOW, we considered to be instantaneous. Therefore, it was used to indicate when the mixing chamber reached the goal concentration and to compare its readings to the SEACOWs' response time. To estimate the air-side response time of the SEACOW, the mixing chamber was flooded with 1500 ppm CO_2 until both the SEACOW and LI-850 stabilized. At a recorded time, the top of the box was removed and the box was flooded with ambient air, facilitated by a fan. The time it took for each instrument to stabilize to the influx of ambient air was recorded, which provides an approximation of 5τ, or 99.3% response time, for the air-side.

To estimate the 5τ time for the water-side, a gas mixture of 1000 ppm CO_2 was bubbled into 2 L of deionized water for 24 h to produce water with elevated pCO_2. A stir plate was used to ensure even mixing. Additionally, the gas mixture was bubbled first through a flask of deionized water prior to reaching the 2 L to humidify the gas stream and reduce evaporation. We placed the SEACOW into the 2 L of high pCO_2 water and recorded the amount of time it took for the SEACOW to completely equilibrate as an estimate of the water-side 5τ time.

https://doi.org/10.5194/egusphere-2024-3375
Preprint. Discussion started: 6 November 2024
© Author(s) 2024. CC BY 4.0 License.

2.2.3 Humidity and pressure correction

We used the humidity, pressure, and temperature measurements from the BME280 sensor inside the K30 housing, as well as the water/air-side temperatures, to correct our K30 readings following methods by Wall (2014), which we've updated for our lower humidity air stream:

$$K30_{CO2} = [(K30_{raw} - K30_{H2O}) * m_{dry}] + b \quad (2)$$

$$K30_{H2O} = (m_{H2O} * V_{H2O} + b_{H2O}) * (H/100) \quad (3)$$

$$V_{H2O} = 6 * 10^{-5}(T^3) + 5 * 10^{-4}(T^2) + 0.055(T) + 0.571 \quad (4)$$

In these equations, $K30_{CO2}$ is the corrected CO_2 reading, $K30_{raw}$ is the reading before correction, $K30_{H2O}$ is the amount of the reading due to the presence of water vapor, m_{dry} and b are the slope and intercept of the dry calibration curve (as described in the above Sect. 2.2.1), m_{H2O} and b_{H2O} are the slope and intercept of the K30 reading vs vapor pressure curve linear regression, H is the relative humidity inside the K30 housing, V_{H2O} is the vapor pressure of water, and T is the water temperature in °C.

To obtain m_{H2O} and b_{H2O} first, a flask of deionized water was placed inside a water bath (6200 R20, Fisher Scientific, MA, USA) through which we bubbled pure N_2 gas to achieve a 100% humidity airstream which fed into the K30 housing. The temperature of the water was varied from 18–24 °C to simulate a reasonable temperature range for the coast of North Carolina and then vapor pressure was calculated according to Eq. (4). Once the vapor pressure values were calculated, a linear fit between vapor pressure and the K30 readings resulted in m_{H2O} and b_{H2O} of -3.2 and 45 µatm, respectively. Note that no CO_2 gas was used in this step, so the entire response is due to H_2O.

This vapor pressure was calculated at a 100% humidity stream, but the inside the K30 housing only gets to 40–50% humidity during deployments due to the Nafion tubing and Drierite. Therefore, we multiply $K30_{H2O}$ by the proportion of the logged humidity to account for the fact that 100% humidity is not reached during actual deployments.

2.3 Laboratory seagrass experiment

A laboratory tank study was conducted in October 2023 to evaluate SEACOW's ability to capture diel pCO_2 cycling. Two tanks (one "experimental" and one "control") were used as follows. For the experimental tank, approximately 0.65 m^2 of *Halodule wrightii* was collected from a seagrass bed at 34.398° N, 77.616° W in September 2023 under UNCW CMS Collection DMF Permit #2037980 by coring the area to preserve the root system of the seagrass. Immediately following the coring, the seagrass and its sediment were placed into 4 rectangular plastic containers and placed into coolers, which were filled with seawater to avoid desiccation. Additionally, ≈ 45 L of sediment were collected from a seagrass-free area. The seagrass was placed in the experimental tank within 4 hours of collection after its plastic container was further filled with the collected sediment to make sure it was securely planted. Sand (collected at 34.1934° N, 77.8047° W) was also sprinkled on top of the muddy sediment to decrease resuspension. The 95 L tank was filled with filtered seawater (<10 µm) to decrease the amount of biologically active material (i.e., living heterotrophs or autotrophs which could influence CO_2 and O_2) in the tank.

https://doi.org/10.5194/egusphere-2024-3375
Preprint. Discussion started: 6 November 2024
© Author(s) 2024. CC BY 4.0 License.

For the control tanks, four more empty plastic containers were filled with the collected sediment and sand and placed in a different 95 L tank, which was also filled with the same filtered seawater.

Each tank was outfitted with a hanging power filter (Qmax 90GPH), without the filter, to gently mix the water and a glass tank heater set to 22 ℃ which is within the thermal optimal for *H. wrightii* (Mazzotti et al., 2007). Because the tanks were closed loop systems and prone to evaporation, about 4 L of deionized water were added every 2–3 days to ensure the salinity of the tanks stayed consistently at 34–36 PSU. *H. wrightii* tolerates a wide range of salinities, from 25–45 PSU, with no changes in growth rate; therefore, it was kept at an optimal range similar to where it was collected from (Mazzotti et al., 2007). Four Finnex Planted+ aquarium lights were put on each tank to ensure sufficient lighting and were on from 6 am to 6 pm every day. One SEACOW and one dissolved oxygen (DO) sensor (miniDOT, PME, CA, USA) were placed in each tank. The SEACOW measured atmospheric pCO_2 for 8 min and then switched to sampling aquatic pCO_2 for 60 min at rate of 0.5 Hz. After sampling, it entered sleep mode for 52 min; consequently, one atmospheric and one aquatic pCO_2 value is measured every two hours. The dissolved oxygen sensor sampled every 2 min continuously. We then averaged the last 5 and 3 minutes of raw data for each water-side and air-side cycle, respectively, which are the equilibrated end points reported in the results.

Ten discrete water samples were also collected from each tank throughout the laboratory seagrass experiment to analyze dissolved inorganic carbon (DIC) and total alkalinity (TA). Before beginning collection, 20 mL glass scintillation vials were pre-poisoned with 10 µL of saturated mercuric chloride to prevent any biologic activity in the water samples that would affect the DIC or TA. Next, we took the plunger out of a 60 mL syringe, rinsed both parts in the water being sampled three times, and gently dipped it underwater to fill. We added the plunger while it was underwater to avoid any great pressure changes that could affect the TA/DIC. After lifting it out of the water, we added a tubing attachment to the syringe, dispensed 10 mL to rinse the inside of the tubing, and then put the tubing at the bottom of the 20 mL scintillation bottle and slowly started filling the vial to the very top for the DIC sample. The tubing attachment allows the water to gently flow into the vial to reduce gas exchange which would alter the DIC (and pCO_2) value. Keeping the same water in the syringe, we then switched the tubing attachment for an Acrodisc GxF/Glass 25 mm filter, dispensed 10 mL to rinse the filter and then filled the vial to the top for the TA sample. This process was repeated two more times with different syringes for each tank, so each sample was taken in triplicate. Immediately following sampling, parafilm was wrapped clockwise around the tops of the vials to prevent evaporation. Salinity and temperature measurements were taken with a Castaway CTD (SonTek, California, USA). TA samples were analyzed using an 848 Titrino Plus autotitrator (Metrohm, Switzerland). DIC was measured using a Shimadzu organic carbon analyzer which also provides the DIC fraction, though with known inaccuracy larger than needed for climate quality marine inorganic carbon measurements (Newton et al., 2015; Tamura, 2023).

After obtaining TA and DIC values, we used the seacarb package in RStudio to calculate pCO_2 values, using the temperature and salinity data taken at the time of collection (Gattuso et al., 2021). We then compared those pCO_2 values to the equilibrated water pCO_2 values from the SEACOW.

https://doi.org/10.5194/egusphere-2024-3375
Preprint. Discussion started: 6 November 2024
© Author(s) 2024. CC BY 4.0 License.

3 Results

3.1 Response time of different membranes

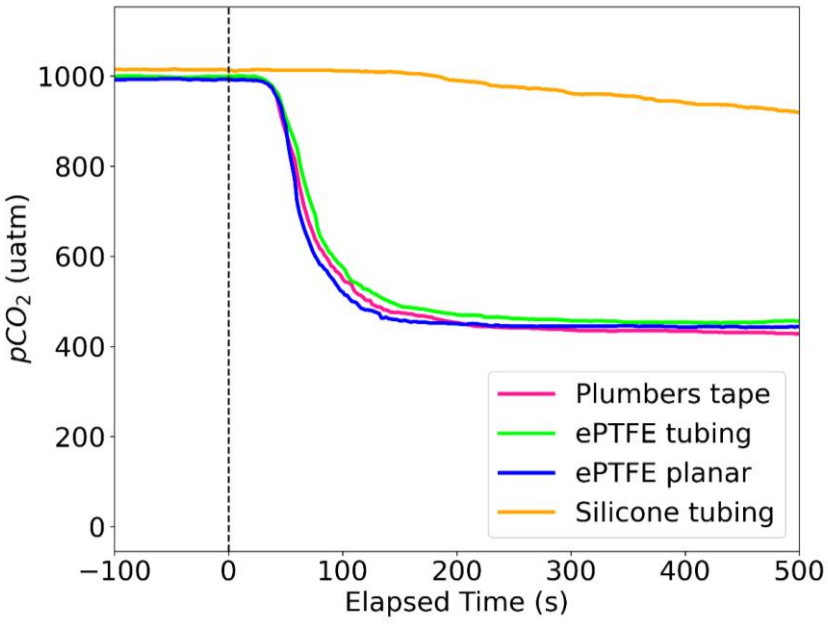

Figure 3. Response time of several semipermeable membranes to a change in pCO_2 occurring at time 0.

During the development process, the response time of several different potential diffusion membranes was evaluated by flooding a chamber with a known concentration of CO_2 and observing their response (Figure 3). The ePTFE (tubing 250 µm thick; planar 900 µm thick) had one of the fastest response times and higher durability than regular PTFE plumber's tape (approx. 80 µm thick), so we chose it for our diffusion membranes. The silicone tubing we tested had a wall thickness of about 280 µm.

3.2 Air and water-side response time

The averaged 99.3% air-side response time, or 5τ, of the SEACOW is 5.7 min, which was estimated by recording the amount of time it took for the SEACOWs to nearly equilibrate to the ambient air (Figure 4A). Therefore, 1τ is 1.14 minutes. It appears that there is not just a diffusion-limited response time, but also a lag, likely due to "dead volume" in the system that needs to be flushed. It is important to note that the LI-850 did not have any diffusive barrier in place during this experiment and pumps at a rate of 0.75 liters per minute. On the other hand, the SEACOW had the ePTFE planar diffusive membrane and

https://doi.org/10.5194/egusphere-2024-3375
Preprint. Discussion started: 6 November 2024
© Author(s) 2024. CC BY 4.0 License.

pumps at a rate of about 0.20 liters per minute. Note that SEACOW2 became inoperable and is therefore excluded from the results.

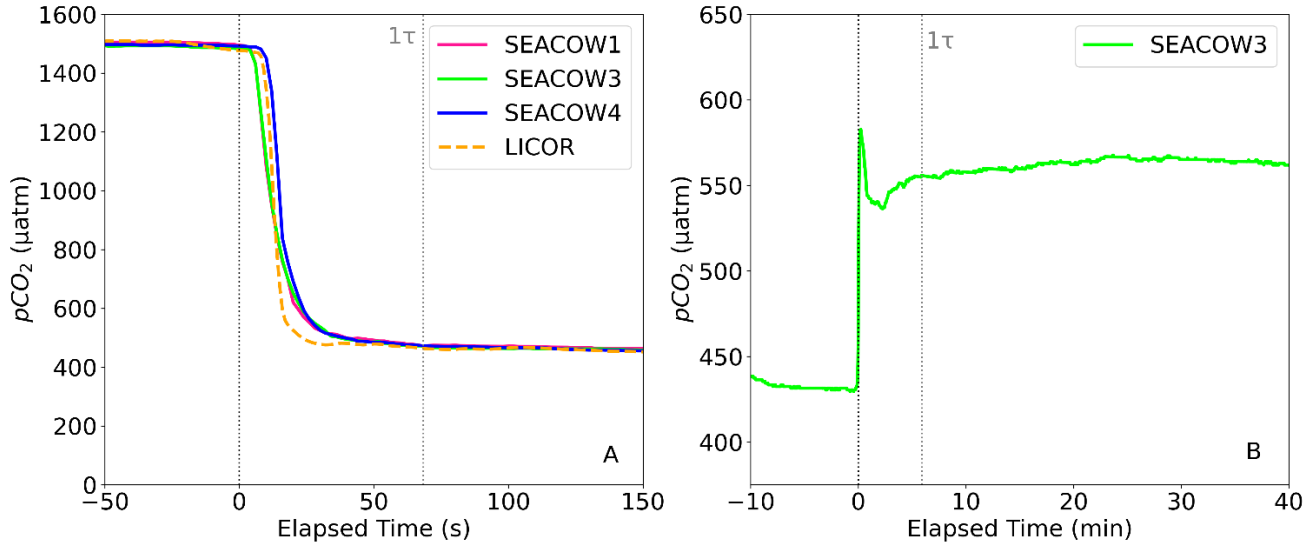

Figure 4. A: The response of the SEACOWs air-side to a step change of pCO_2 occurring at time 0. Note the x-axis has been limited to 150 seconds in order to emphasize the response within 1τ, as opposed to the full 5τ response. B: The response of the SEACOW to a step change in aquatic pCO_2 at time 0.

Water-side response time (5τ) was calculated to be 29.6 minutes (Figure 4B). The equilibration of the water-side is less stable than that of the air -side, with a large spike in the data occurring immediately after being placed in the water which could be the result of a pressure change. The general instability in the water-side response curve is likely caused by imperfections with our testing tank – the 2L container of DI water was open to the atmosphere while being bubbled with our gas mixture on a stir plate, potentially leading to small changes in aquatic pCO_2 happening faster than the SEACOW could measure. Additionally, the diffusion of CO_2 through water is slower than air, further contributing to the lag between the real time conditions and what the SEACOW was measuring.

3.3 Air-side accuracy

A stepwise gas experiment was conducted to assess variations in K30 (and therefore SEACOW) performance "out of the box" and after calibration. Both pre and post-calibration, the SEACOWs had standard deviations < 3 µatm (typically < 1 µatm), demonstrating the instruments' stability across the full range sampled (Table 1).

Table 1. Summary of results from air-side dry calibration stepwise gas experiment. Pre refers to values that have not been calibrated, while post refers to those that have. SEACOW2 became inoperable and thus was excluded from this table. Reported values are the

https://doi.org/10.5194/egusphere-2024-3375
Preprint. Discussion started: 6 November 2024
© Author(s) 2024. CC BY 4.0 License.

mean ± the standard deviation during the last 5 minutes of data at each step. Eqs. (2-4) were applied as part of the calibration process.

Set Point (µatm)	**SEACOW1 Average Reading** (µatm)		**SEACOW3 Average Reading** (µatm)		**SEACOW4 Average Reading** (µatm)		**LI-850 Average Reading** (µatm)
	Pre	*Post*	*Pre*	*Post*	*Pre*	*Post*	
0	94 ± 0.78	-19 ± 0.37	6 ± 0.91	25 ± 0.89	51 ± 0.73	-30 ± 0.54	1.44 ± 0.09
250	369 ± 0.57	230 ± 0.52	208 ± 0.70	233 ± 0.79	298 ± 1.82	219 ± 1.36	238.38 ± 0.20
500	653 ± 0.61	484 ± 0.52	445 ± 0.88	472 ± 0.80	561 ± 1.08	474 ± 1.00	490.90 ± 0.32
750	937 ± 0.87	738 ± 0.76	690 ± 0.98	719 ± 0.94	825 ± 2.42	726 ± 2.21	744.75 ± 0.50
1000	1229 ± 0.61	997 ± 0.49	941 ± 1.37	968 ± 1.30	1097 ± 1.42	985 ± 1.30	999.32 ± 0.59
1500	1798 ± 0.84	1505 ± 0.75	1464 ± 1.42	1493 ± 1.47	1633 ± 2.04	1496 ± 1.91	1508.16 ± 0.72
Dry Calibration Curves: SEACOW1: $K30_{corrected} = 0.89(K30_{raw}) - 86$ SEACOW3: $K30_{corrected} = 1(K30_{raw}) + 40$ SEACOW4: $K30_{corrected} = 0.95(K30_{raw}) - 45$							

After the dry calibration constants were applied (Table 1), SEACOWs reported stabilized measurements to within ~2.5% of the LI-850's readings on average, excluding values at 0 µatm (Figure 5). After calibration, the root mean square errors for SEACOWs 1, 3, and 4 in comparison with LI-850's values are 5.09, 12.13, 3.48 µatm, respectively. Water-side accuracy has not been separately characterized, but, given the use of the same K30 sensing unit for both water and air-side measurements, no difference is expected. Moreover, given that the final measurement is a ΔpCO_2, any offset in pCO_2 calculated from the K30 response should be cancelled out. We acknowledge, however, that difference in sensor gain could contribute to inaccuracy as ΔpCO_2 increases.

https://doi.org/10.5194/egusphere-2024-3375
Preprint. Discussion started: 6 November 2024
© Author(s) 2024. CC BY 4.0 License.

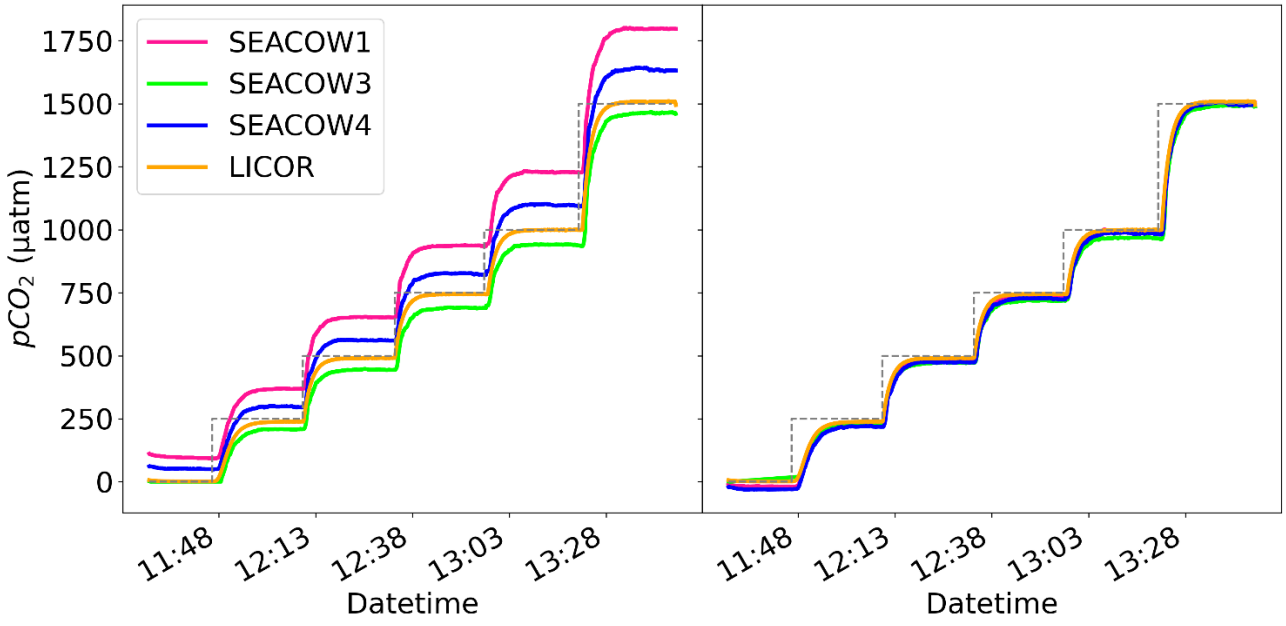

240 **Figure 5. Stepwise gas experiment of all four SEACOWs vs the LI-COR LI-850 before (left) and after (right) the dry calibration curve was applied. LI-COR LI-850 XCO_2 measurements were converted to pCO_2 for comparison.**

3.4 Seagrass tank experiment

https://doi.org/10.5194/egusphere-2024-3375
Preprint. Discussion started: 6 November 2024
© Author(s) 2024. CC BY 4.0 License.

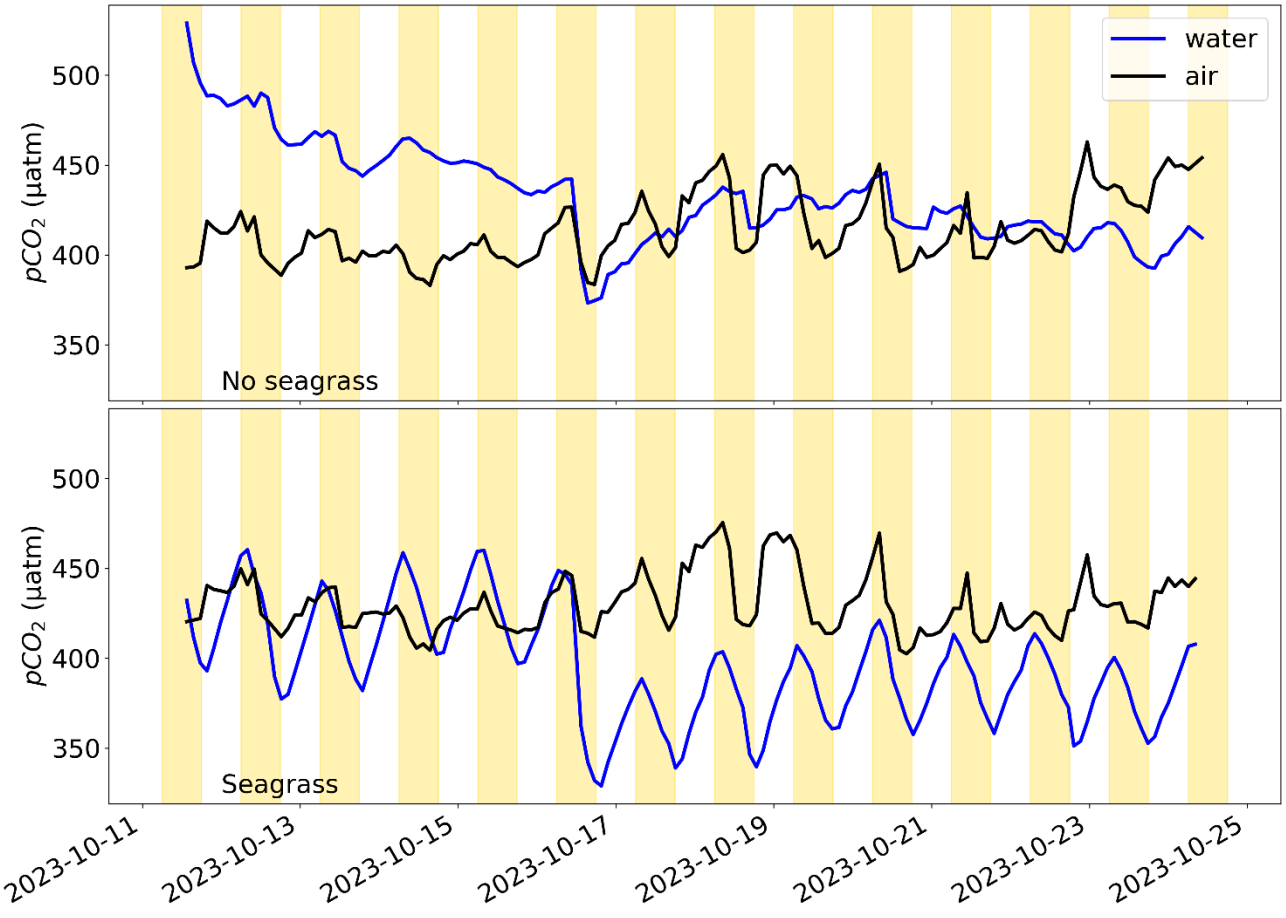

Figure 6. Equilibrated pCO_2 end points plotted for the air (black) and water-side (blue) for the tanks with and without seagrass, as labelled. Yellow background signifies "daytime," or when the aquarium lights are illuminated, and white background signifies "nighttime," or when lights are turned off.

SEACOWs collected ΔpCO_2 data successfully in two tanks for two weeks. SEACOW1 was in the control tank, while SEACOW3 and SEACOW4 were in the seagrass tank. However, values from SEACOW3 are excluded from Figure 6 due to reporting unreliable data, likely caused by an internal air leak. Dissolved oxygen data were especially noisy in the "No Seagrass" tank and are therefore shown in Supplemental Material. We suspect that small air bubbles may have been trapped on the surface of the DO sensor's face. Both tanks (i.e., with and without seagrass) showed evidence of some diel pCO_2 cycling, likely due to the presence of a microbial community in the sediment. However, pCO_2 cycling is much more regular and amplified in the tank with seagrass (Figure 6), indicative of clear photosynthesis–respiration cycles. The lack of cycling in the DO readings in Tank 1 also suggest that there was no consistent photosynthesis happening, presumably due to the lack of seagrass (Figure S1). Initially in the experiment (Oct. 11–16), the atmospheric pCO_2 was unexpectedly rising during the day and falling at night (Figure 6), likely due to other lab users entering the lab during the day and respiring, which would raise

https://doi.org/10.5194/egusphere-2024-3375
Preprint. Discussion started: 6 November 2024
© Author(s) 2024. CC BY 4.0 License.

the atmospheric CO_2 levels. However, around October 16th, this pattern ceased, and the atmospheric and aquatic pCO_2 were rising and falling at the same times of the days. On October 16th, a larger quantity of deionized water was added to the tanks to maintain their salinity, which may have caused the sudden decrease in aquatic pCO_2 levels on that day. However, the addition of deionized water should not have affected the atmospheric pCO_2 cycling, so it is unknown what caused the change.

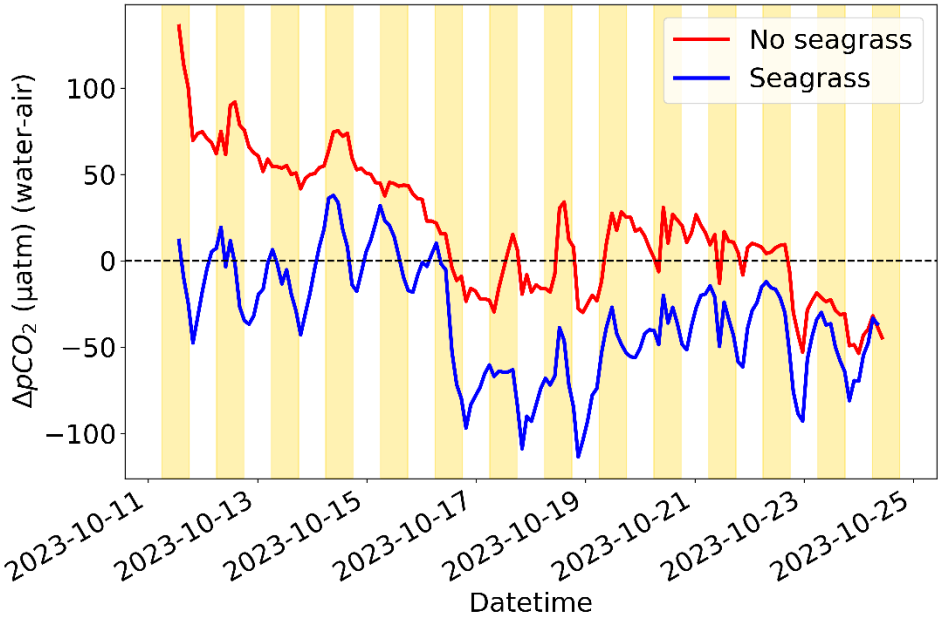

Figure 7. ΔpCO_2 (water-air) values for SEACOW1 and 4, which were in the control tank and seagrass tank, respectively.

For Figure 7, the difference between the averaged equilibrated water-side values and the air-side values were taken to produce ΔpCO_2 values. From October 11th-October 16th, the ΔpCO_2 values were as expected with the seagrass tank seeing more consistent diel cycling with values decreasing throughout the day and increasing through the night. Additionally, because the atmospheric pCO_2 values from both SEACOWs matched closely (Figure 6), most of the differences between the ΔpCO_2 values of each tank can be attributed to the aquatic pCO_2.

Discrete samples were collected for analysis of DIC/TA and estimation of pCO_2. However, severe mismatch between SEACOW and discrete pCO_2, and noise on the order of 10–100 µatm in estimated pCO_2 suggest discrete sample analysis issues that were unable to be resolved in the course of this study. As previously mentioned, only a total organic carbon analyzer was available during this work, and DIC estimations from organic carbon analyzers are known to fall far short of best practices for measurement of DIC (Dickson et al., 2007). We report aquatic pCO_2 measured by both SEACOWs and discrete samples in Figure S2, but these samples are unable to be used to further characterize the instruments.

One of the main results of this project is the creation of the SEACOW itself, for which its characterization data is summarized below:

https://doi.org/10.5194/egusphere-2024-3375
Preprint. Discussion started: 6 November 2024
© Author(s) 2024. CC BY 4.0 License.

Table 2. Summary of the characterization data for the SEACOW

Characterization parameter	***Value***
Accuracy	± 2.5% of LI-850's readings
Air-side 5τ time	5.7 minutes
Water-side 5τ time	~30 minutes
Power draw	185 mW
Drierite budget	162 grams per 5 days
Temperature range	5-40 ℃
Cost in parts	~1400 USD
Github: https://zenodo.org/doi/10.5281/zenodo.13751037	

4 Discussion

Sampling pCO_2 in marine environments can be logistically difficult and expensive, yet it is a critical parameter to monitor as anthropogenic CO_2 continues to change the ocean chemistry. Not only does monitoring pCO_2 give scientists a better understanding of the quantity and effects of anthropogenic CO_2 uptake, but it allows scientists to study many different aspects of oceanography such as the movement of water along the oceanic conveyor belt (Takahashi et al., 2009), the effect pCO_2 concentrations have on calcifying organisms (Fujita et al., 2011), or the productivity of a region (Körtzinger et al., 2008). Additionally, there has been an increase in marine carbon dioxide removal (mCDR) groups who are looking for the best ways to monitor the movement of CO_2, so they can verify their methods of sequestering CO_2 from the atmosphere. Due to labor intensive and expensive methods of high quality pCO_2 sensing, many of these groups and scientists are interested in low-cost pCO_2 technologies that can be deployed in larger quantities alongside more expensive, but singular, pCO_2 systems. In addition to developing pCO_2 monitoring for artificial carbon dioxide removal, it is important to monitor and protect blue carbon habitats that naturally sequester carbon, like seagrass meadows.

During deployments, we also identified several areas of improvement for the SEACOW. Although the response time for the air-side is sufficient for capturing rapid changes in atmospheric CO_2 during deployments, the water-side response time is not as competitive when compared to other pCO_2 instruments. The $SIPCO_2$ (accuracy 29 ± 6 µatm) (Hunt et al., 2017) and the CO2-Pro (accuracy ±0.5%) (Pro-Oceanus) have reported approximate 5τ response times of 15 minutes and 12.5 minutes, respectively. The CO2-Pro's efficient response time could be attributed to its pump that moves water across the equilibration membrane, which also reduces biofouling, but increases its power consumption. The SEACOW's water-side response time could be accelerated by adding an external pump or stirring mechanism, which may also assist in preventing biofouling. Additional research could also focus on improving the exchanger material and/or geometry (i.e., a higher surface area to volume ratio) to assist with CO_2 permeation. We also note that Formlabs does not supply resin chemistry and we therefore do

https://doi.org/10.5194/egusphere-2024-3375
Preprint. Discussion started: 6 November 2024
© Author(s) 2024. CC BY 4.0 License.

not know what its CO_2 permeability/absorptivity properties are. However, given these results, especially on the air-side, we do not consider this to be a significant source of uncertainty or response time lag.

Finally, for the SEACOW to be used as an autonomous field instrument, the most pressing improvements for future deployments are the addition of a solar panel or larger battery pack, adding more Drierite to the system/using a different drying mechanism, and decreasing biofouling. These advancements would allow the SEACOW to be deployed alongside more robust systems to increase spatial resolution of sampling.

5 Conclusions

In this project, we designed and built a ΔpCO_2 device, characterized its functionality, and demonstrated its ability to capture the diel pCO_2 cycling of seagrass in a controlled environment. The increasing popularity of microcontrollers and off-the-shelf parts help improve accessibility of monitoring technologies, which was one of the major goals of this project. During our seagrass tank deployment, we demonstrated the capability of the SEACOW to capture diel cycling of pCO_2. In the future, work will be focused on characterizing water-side accuracy, decreasing water-side response time, and making the instrument more robust for field deployments. The work presented here further aids in characterizing the K30, which is increasingly popular in other low-cost atmospheric and/or aquatic CO_2-sensing technologies. Because the SEACOW measures atmospheric and aquatic pCO_2, a ΔpCO_2 ($pCO_{2(water)}$-$pCO_{2(air)}$) value can be obtained and used to calculate CO_2 fluxes. Therefore, even if the K30 sensor readings start to drift over time, the drift is subtracted out when the difference is taken, allowing the SEACOW to maintain rigor during deployments. This feature, along with the fact that the parts cost ~1,400 USD, make the SEACOW a valuable contribution to biogeochemical scientific and engineering communities.

6 Appendices

Appendix A.

All electrical components were purchased off the shelf and soldered onto a breadboard. The firmware to control the SEACOW was developed in Visual Studio Code using the Particle extension and included libraries. An overview of each component and its purpose is given below the following circuit diagram:

https://doi.org/10.5194/egusphere-2024-3375
Preprint. Discussion started: 6 November 2024
© Author(s) 2024. CC BY 4.0 License.

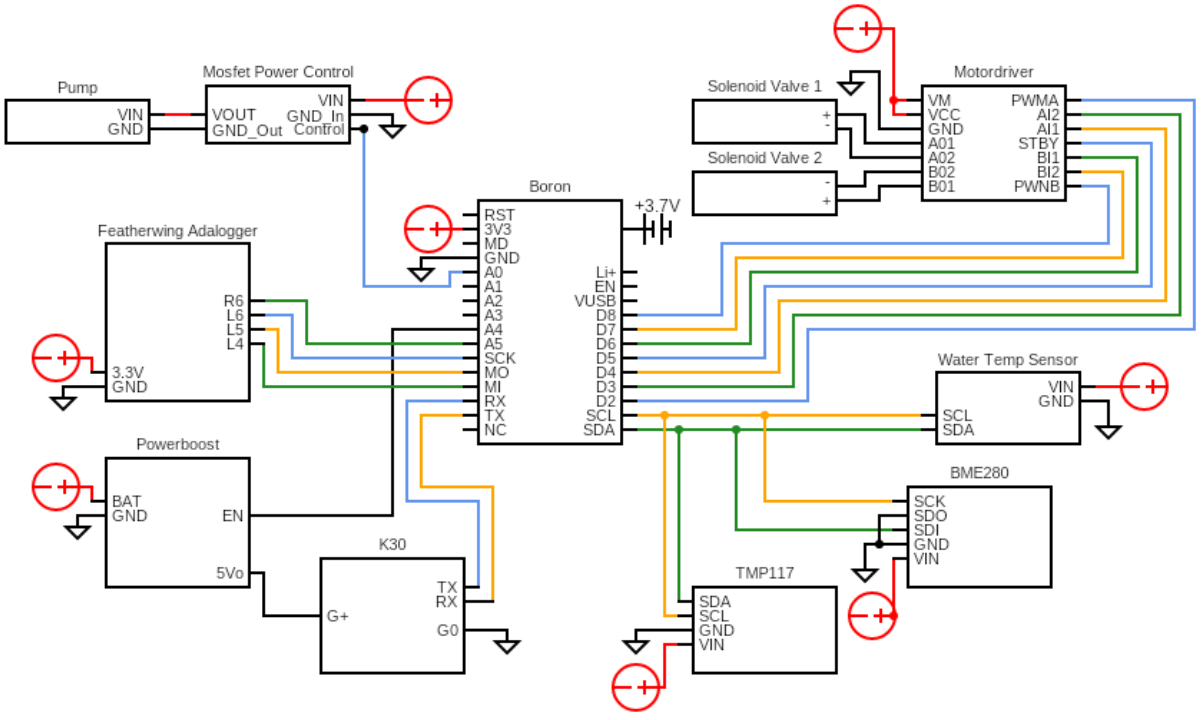

Figure A1. Circuit diagram of the electrical components of the SEACOW

1. Particle Boron (BRN404XKIT): the microcontroller that carries out the commands from the firmware. The Boron has an onboard cellular modem with LTE capabilities, allowing it to upload data directly to a google spreadsheet during its deployments. It is powered using a rechargeable 3.7 V Li-ion battery.
2. Lee Co 3-way solenoid valves (LHLA0531211H): controls the flow of air to switch between measuring the air-side and the water-side of the instrument.
3. Sparkfun motordriver (ROB-14450): controls the solenoid valves.
4. Blue Robotics temperature sensor (BR-100317): measures the water temperature.
5. Adafruit BME 280 sensor (2652): measures temperature, pressure, and humidity inside of the K30 housing.
6. Adafruit TMP 117 sensor (4821): measures the temperature on the air-side of the instrument.
7. Senseair K30 CO_2 sensor (030-8-0006): the NDIR sensor that is measuring pCO_2.
8. Adafruit Powerboost (1944): converts the 3.3 V output of the Boron to a 5 V output, which is the minimum voltage required for the K30 to function. It also turns on and off the K30 during sleeping periods.
9. Adafruit Adalogger Featherwing (2922): the datalogger that stores data onto its SD card.
10. Diaphragm gas pump (UNMP 05): moves the air throughout the closed loop system.
11. Sparkfun MOSFET power control kit (COM-12959): allows us to turn the pump on and off in between samples.

https://doi.org/10.5194/egusphere-2024-3375
Preprint. Discussion started: 6 November 2024
© Author(s) 2024. CC BY 4.0 License.

Appendix B.

CO_2 Mass flow controller calculations:

$$M_{N2} = Molar\ flow\ rate\ for\ N_2 \left(\frac{mol}{min}\right) = \frac{P*MFC_{N2}}{R*T} \quad \text{(B1)}$$

$$M_{CO2} = Molar\ flow\ rate\ for\ CO_2 \left(\frac{mol}{min}\right) = \frac{C*10^{-6}*M_{N2}}{1-C*10^{-6}} \quad \text{(B2)}$$

$$MFC_{CO2}(Lpm) = \frac{R*T*M_{CO2}}{P} \quad \text{(B3)}$$

Where the assumed constants are:

T = Temperature = 296.15 K
R = 0.0821 (L atm mol^{-1} K^{-1})
P = Room pressure = 1 atm
C = Desired CO_2 concentration in ppm
MFC_{N2} = Mass flow controller for N_2 is set at 5 Lpm.

7 Code and data availability

https://zenodo.org/doi/10.5281/zenodo.13751037

8 Author contribution

EF conceptualized the device, the methodology, and the experiments and carried out the investigation. PB conceptualized the device and provided support throughout all stages of the project, including methodology, investigation, and resources. PB and EF analyzed data. EF wrote the manuscript draft. PB reviewed and edited the manuscript. RW and JJ provided support during the investigation, helped curate the methodology, and assisted with resources. MT and DP furthered in carrying out the investigation.

9 Competing interests

The authors declare that they have no conflict of interest.

10 Acknowledgments

This work was supported by UNC Wilmington's Department of Earth and Ocean Sciences, the College of Arts and Sciences, and the Office of Innovation and Commercialization via a Blue Economy Grant. Sunburst Sensors supported EF through NOAA SBIR grant (NA22OAR0210490). We would also like to thank Bentley Settin and Russ Isobe for their help in the field

https://doi.org/10.5194/egusphere-2024-3375
Preprint. Discussion started: 6 November 2024
© Author(s) 2024. CC BY 4.0 License.

and support in the lab; and Sophia Hill and Luke Cooper for building additional SEACOW units and their buoy systems. Many thanks to John Nunes, Dave Wells, and Jimmy White for providing support to lab and field testing of the SEACOW.

11 References

Bauer, J. E., Cai, W.-J., Raymond, P. A., Bianchi, T. S., Hopkinson, C. S., and Regnier, P. A. G.: The changing carbon cycle of the coastal ocean, Nature, 504, 61-70, 10.1038/nature12857, 2013.

Bresnahan Jr, P. J., Martz, T. R., Takeshita, Y., Johnson, K. S., and LaShomb, M.: Best practices for autonomous measurement of seawater pH with the Honeywell Durafet, Methods in Oceanography, 9, 44-60, https://doi.org/10.1016/j.mio.2014.08.003, 2014.

Dai, M., Su, J., Zhao, Y., Hofmann, E. E., Cao, Z., Cai, W.-J., Gan, J., Lacroix, F., Laruelle, G. G., Meng, F., Müller, J. D., Regnier, P. A. G., Wang, G., and Wang, Z.: Carbon Fluxes in the Coastal Ocean: Synthesis, Boundary Processes, and Future Trends, Annual Review of Earth and Planetary Sciences, 50, 593-626, 10.1146/annurev-earth-032320-090746, 2022.

Dickson, A. G., Sabine, C. L., and Christian, J. R.: Guide to best practices for ocean CO2 measurements, North Pacific Marine Science Organization2007.

Fourqurean, J. W., Duarte, C. M., Kennedy, H., Marbà, N., Holmer, M., Mateo, M. A., Apostolaki, E. T., Kendrick, G. A., Krause-Jensen, D., Mcglathery, K. J., and Serrano, O.: Seagrass ecosystems as a globally significant carbon stock, Nature Geoscience, 5, 505-509, 10.1038/ngeo1477, 2012.

Friedlingstein, P., O'sullivan, M., Jones, M. W., Andrew, R. M., Gregor, L., Hauck, J., Le Quéré, C., Luijkx, I. T., Olsen, A., and Peters, G. P.: Global carbon budget 2022, Earth System Science Data, 14, 4811-4900, https://doi.org/10.5194/essd-14-4811-2022, 2022.

Fujita, K., Hikami, M., Suzuki, A., Kuroyanagi, A., Sakai, K., Kawahata, H., and Nojiri, Y.: Effects of ocean acidification on calcification of symbiont-bearing reef foraminifers, Biogeosciences, 8, 2089-2098, https://doi.org/10.5194/bg-8-2089-2011, 2011.

Gattuso, J.-P., Epitalon, J.-M., Lavigne, H., and Orr, J.: seacarb: seawater carbonate chemistry [code], 2021.

Ge, X., Kostov, Y., Henderson, R., Selock, N., and Rao, G.: A low-cost fluorescent sensor for pCO2 measurements, chemosensors, 2, 108-120, https://doi.org/10.3390/chemosensors2020108, 2014.

Graziani, S., Beaubien, S. E., Bigi, S., and Lombardi, S.: Spatial and temporal pCO2 marine monitoring near Panarea Island (Italy) using multiple low-cost GasPro sensors, Environmental science & technology, 48, 12126-12133, https://doi.org/10.1021/es500666u, 2014.

Herr, D. and Landis, E.: Coastal blue carbon ecosystems. Opportunities for Nationally Determined Contributions. Policy Brief, 2016.

Hunt, C. W., Snyder, L., Salisbury, J. E., Vandemark, D., and Mcdowell, W. H.: SIPCO2: A simple, inexpensive surface water pCO2 sensor, Limnology and Oceanography: Methods, 15, 291-301, 10.1002/lom3.10157, 2017.

Johnson, M. S., Billett, M. F., Dinsmore, K. J., Wallin, M., Dyson, K. E., and Jassal, R. S.: Direct and continuous measurement of dissolved carbon dioxide in freshwater aquatic systems-method and applications, Ecohydrology, 68-78, 10.1002/eco.95, 2009.

Körtzinger, A., Send, U., Lampitt, R., Hartman, S., Wallace, D. W., Karstensen, J., Villagarcia, M., Llinás, O., and DeGrandpre, M.: The seasonal pCO2 cycle at 49 N/16.5 W in the northeastern Atlantic Ocean and what it tells us about biological productivity, Journal of Geophysical Research: Oceans, 113, https://doi.org/10.1029/2007JC004347, 2008.

Lefèvre, N., Watson, A. J., Cooper, D. J., Weiss, R. F., Takahashi, T., and Sutherland, S. C.: Assessing the seasonality of the oceanic sink for CO2 in the northern hemisphere, Global Biogeochemical Cycles, 13, 273-286, https://doi.org/10.1029/1999GB900001, 1999.

Macreadie, P., Baird, M., Trevathan-Tackett, S., Larkum, A., and Ralph, P.: Quantifying and modelling the carbon sequestration capacity of seagrass meadows–a critical assessment, Marine pollution bulletin, 83, 430-439, https://doi.org/10.1016/j.marpolbul.2013.07.038, 2014.

https://doi.org/10.5194/egusphere-2024-3375
Preprint. Discussion started: 6 November 2024
© Author(s) 2024. CC BY 4.0 License.

Martin, C. R., Zeng, N., Karion, A., Dickerson, R. R., Ren, X., Turpie, B. N., and Weber, K. J.: Evaluation and environmental correction of ambient CO2 measurements from a low-cost NDIR sensor, Atmospheric measurement techniques, 10, 2383-2395, https://doi.org/10.5194/amt-10-2383-2017, 2017.

Mazzotti, F. J., Pearlstine, L. G., Chamberlain, R., Barnes, T., Chartier, K., and DeAngelis, D.: Stressor response models for Seagrasses, Halodule wrightii and Thalassia testudnium., University of Florida, Florida Lauderdale Research and Education Center, Fort Lauderdale, Florida, 19, 2007.

Newton, J., Feely, R., Jewett, E., Williamson, P., and Mathis, J.: Global ocean acidification observing network: requirements and governance plan, 2015.

Nicholson, D. P., Michel, A. P. M., Wankel, S. D., Manganini, K., Sugrue, R. A., Sandwith, Z. O., and Monk, S. A.: Rapid Mapping of Dissolved Methane and Carbon Dioxide in Coastal Ecosystems Using the ChemYak Autonomous Surface Vehicle, Environmental Science & Technology, 52, 13314-13324, 10.1021/acs.est.8b04190, 2018.

Pan, C., Patel, V., Gewirtzman, J., Richardson, I., Dubey, R., Caylor, K., Dollar, A., and Forbes, E.: Fluxbot: The Next Generation-Design and Validation of a Wireless, Open-Source Mechatronic CO2 Flux Sensing Chamber, Proceedings of the 7th ACM SIGCAS/SIGCHI Conference on Computing and Sustainable Societies, 85-96, https://doi.org/10.1145/3674829.3675063,

Resplandy, L., Hogikyan, A., Müller, J., Najjar, R., Bange, H. W., Bianchi, D., Weber, T., Cai, W. J., Doney, S., and Fennel, K.: A synthesis of global coastal ocean greenhouse gas fluxes, Global Biogeochemical Cycles, 38, e2023GB007803, https://doi.org/10.1029/2023GB007803, 2024.

Rosentreter, J. A.: Water-air gas exchange of CO2 and CH4 in coastal wetlands, in: Carbon Mineralization in Coastal Wetlands, Elsevier, 167-196, https://doi.org/10.1016/B978-0-12-819220-7.00003-0, 2022.

Sabine, C., Sutton, A., Mccabe, K., Lawrence-Slavas, N., Alin, S., Feely, R., Jenkins, R., Maenner, S., Meinig, C., Thomas, J., Van Ooijen, E., Passmore, A., and Tilbrook, B.: Evaluation of a New Carbon Dioxide System for Autonomous Surface Vehicles, Journal of Atmospheric and Oceanic Technology, 37, 1305-1317, 10.1175/jtech-d-20-0010.1, 2020.

Senseair of Delsbo, S.: Modbus on Senseair K30, Senseair K33 and eSENSE - Document TDE2336, 2023.

Sutton, A. J., Sabine, C. L., Maenner-Jones, S., Lawrence-Slavas, N., Meinig, C., Feely, R. A., Mathis, J. T., Musielewicz, S., Bott, R., Mclain, P. D., Fought, H. J., and Kozyr, A.: A high-frequency atmospheric and seawater pCO2 data set from 14 open-ocean sites using a moored autonomous system, Earth System Science Data, 6, 353-366, 10.5194/essd-6-353-2014, 2014.

Takahashi, T., Olafsson, J., Goddard, J. G., Chipman, D. W., and Sutherland, S.: Seasonal variation of CO2 and nutrients in the high-latitude surface oceans: A comparative study, Global Biogeochemical Cycles, 7, 843-878, 1993.

Takahashi, T., Sutherland, S. C., Wanninkhof, R., Sweeney, C., Feely, R. A., Chipman, D. W., Hales, B., Friederich, G., Chavez, F., and Sabine, C.: Climatological mean and decadal change in surface ocean pCO2, and net sea–air CO2 flux over the global oceans, Deep Sea Research Part II: Topical Studies in Oceanography, 56, 554-577, https://doi.org/10.1016/j.dsr2.2008.12.009, 2009.

Tamura, Y.: Evaluation of Dissolved Inorganic Carbon in Seawater, 2023.

Wall, C. M.: Autonomous in situ measurements of estuarine surface PCO_2: instrument development and initial estuarine observations, 2014.

Wanninkhof, R.: Relationship between gas exchange and wind speed over the ocean, J. Geophys. Res., 97, 7373-7381, https://doi.org/10.1029/92JC00188, 1992.

Wanninkhof, R., Asher, W. E., Ho, D. T., Sweeney, C., and McGillis, W. R.: Advances in quantifying air-sea gas exchange and environmental forcing, Annual review of marine science, 1, 213-244, https://doi.org/10.1146/annurev.marine.010908.163742, 2009.

Watson, A. J., Schuster, U., Shutler, J. D., Holding, T., Ashton, I. G., Landschützer, P., Woolf, D. K., and Goddijn-Murphy, L.: Revised estimates of ocean-atmosphere CO2 flux are consistent with ocean carbon inventory, Nature communications, 11, 4422, 2020.

Yasuda, T., Yonemura, S., and Tani, A.: Comparison of the Characteristics of Small Commercial NDIR CO2 Sensor Models and Development of a Portable CO2 Measurement Device, Sensors, 12, 3641-3655, 10.3390/s120303641, 2012.